A Method for the Analytical Extraction of the Single-Diode PV Model Parameters

Efstratios I. Batzelis, *Student Member, IEEE*, Stavros A. Papathanassiou, *Senior Member, IEEE*

***Abstract*— Determination of PV model parameters usually requires time consuming iterative procedures, prone to initialization and convergence difficulties. In this paper, a set of analytical expressions is introduced to determine the five parameters of the single-diode model for crystalline PV modules at any operating conditions, in a simple and straightforward manner. The derivation of these equations is based on a newly found relation between the diode ideality factor and the open circuit voltage, which is explicitly formulated using the temperature coefficients. The proposed extraction method is robust, cost-efficient and easy-to-implement, as it relies only on datasheet information, while it is based on a solid theoretical background. Its accuracy and computational efficiency is verified and compared to other methods available in the literature through both simulation and outdoor measurements.**

***Index Terms*—Direct calculation, explicit expressions, five parameters, ideality factor, Lambert W, photovoltaic (PV), single-diode model, temperature coefficients.**

NOMENCLATURE

a	Modified diode ideality factor of the single-diode model.
a_{Isc}	Temperature coefficient of short circuit current.
β_{Voc}	Temperature coefficient of open circuit voltage.
δ	Coefficient for the single-diode model, defined as the ratio of a over V_{oc}.
E_g	Energy gap.
I_{mp}	Current at maximum power point.
I_{ph}	Photocurrent of the single-diode model.
I_s	Diode saturation current of the single-diode model.
I_{sc}	Short-circuit current.
k	Boltzmann constant.
MPP	Maximum power point.
n	Diode ideality factor of the single-diode model.
N_s	Series connected cells in a PV unit.
OC	Open-circuit condition.
q	Electron charge.
R_s	Series resistance of the single-diode model.
R_{sh}	Shunt resistance of the single-diode model.
SC	Short-circuit condition.
STC	Standard test conditions (1000 W/m^2, 25°C).
T_0	Cell temperature at standard test conditions (25°C).
T_c	Operating cell temperature.
V_{mp}	Voltage at maximum power point.
V_{oc}	Open-circuit voltage.
V_{th}	Thermal voltage.
w	Auxiliary parameter related to δ through $w = W\left\{e^{1/\delta+1}\right\}$.
ΔT_c	Deviation of the actual cell temperature from T_0.
X_0	Generic parameter X at STC (e.g. a_0 or V_{oc0}).

I. INTRODUCTION

MODELING of photovoltaic (PV) systems is essential for assessing their efficiency and performance under various operating conditions. Usually, PV modeling is based on a suitable electrical equivalent circuit, employing a set of parameters that represent the properties of the PV modules and the operating conditions. Determination of these parameters is not a trivial task, since they are not generally directly provided in the module datasheet. Numerous methods can be found in the relevant literature for their evaluation, presenting widely different levels of accuracy, computational complexity and amount of required input data. A review of such methods, focusing on energy models for partial shading conditions, is presented in [1].

The majority of these approaches identifies the parameters at standard test conditions (STC), extrapolating then to the actual operating conditions using module datasheet information. With *numerical methods*, a system of equations is formed for specific operating points, which is then solved via a numerical or iterative algorithm [2]–[23]. A representative method of this category is introduced in [2], employing a system of five equations to determine the five parameters of the single-diode model. In particular, the fundamental equation of the model is evaluated at the short-circuit (SC), open-circuit (OC) and maximum power point (MPP), information always given in the module datasheet, while the slope of the *P-V* curve at the MPP is set to zero. The fifth equation is formed by exploiting the linear dependence of the open-circuit voltage on the operating temperature, utilizing the relevant temperature coefficient, also provided in the module datasheet. Similarly, the methods of [3]–[13], [18], [20], [21] rely only on datasheet information, whereas other methods require also the *I-V* curve slope at the SC and/or OC points [14]–[16], [19], or even the entire *I-V* curve [17], [22], [23]. A literature review and comparison through measurements on

Manuscript received May 17, 2015; revised October 10, 2015. Mr. Efstratios Batzelis is supported for his PhD studies by "IKY Fellowships of Excellence for Postgraduate Studies in Greece - Siemens Program".

The authors are with the School of Electrical and Computer Engineering, National Technical University of Athens, Athens 15780, Greece (e-mail: batzelis@mail.ntua.gr; st@power.ece.ntua.gr).

this type of methods can be found in [24] and [25] respectively.

An alternative approach to determine the model parameters is to employ a *curve fitting* or *optimization* algorithm, assuming that the entire *I-V* curve is available. The least-squares fitting technique is applied to measured data in [26]–[29], while various metaheuristic algorithms have been proposed in the literature, implementing genetic algorithms [30], neural networks [31], pattern search [32], particle swarm optimization [33], differential evolution [34] or bird mating optimization [35] algorithms. A comprehensive review and comparative assessment of such methods may be found in [36].

Although all previous methods may provide sufficiently accurate results, they suffer from the iterative nature of the calculation procedure involved. Several computational issues arise, such as initialization difficulties, convergence failure, calculation uncertainty and increased computational cost and complexity. In order to overcome these shortcomings, a few *analytical* methods are proposed in the literature, introducing straightforward techniques to estimate model parameters in an explicit manner, avoiding iterative procedures, albeit at the cost of reduced accuracy [37]–[47]. In [37], the series and shunt resistances of the single diode model are neglected and the remaining three model parameters are derived under the assumption that the slope of the *I-V* curve at the MPP is equal to the ratio of open-circuit voltage to short-circuit current. The shunt resistance is also ignored in [38], leading to direct expressions for the four parameters through various simplifications. The same equations are the outcome of the analysis in [46], while neglecting the shunt resistance in [47] permits determination of the remaining parameters using real-time measurements at six operating points. An interesting method is introduced in [39], which assumes that the shunt and series resistances are equal to the *I-V* curve slope at the SC and OC points respectively, having the latter analytically estimated via the four-parameter model, since these slopes are not available in the module datasheet.

On the other hand, if the slopes at the SC and OC points are known from measurements, the approach of [40] may be applied, which was chronologically the first method to directly determine the five parameters of the single-diode model. The same equations are adopted in [48] and [49], while other approaches may be found in [41]–[43] that also require the measured slopes at the SC and/or OC points. In [44] and [45], additional operating points, apart from the SC, MPP and OC, are required to employ the models proposed therein. Among the explicit methods presented above, only those of [37]–[39] are solely dependent on module datasheet information, however they suffer from reduced accuracy, as shown in this paper.

Objective of this study is to introduce an analytical method to determine the five parameters of the single-diode model of crystalline modules, in an accurate and straightforward manner, using only datasheet information. For this purpose, the widely accepted system of five equations used in [2] is adopted and properly manipulated, leading to simple explicit expressions for the five parameters. This is achieved by exploiting an inherent relation of the diode ideality factor to the open-circuit voltage and the temperature coefficients, introduced for the first time in the literature, which permits expressing the former as an explicit function of the latter. In addition, the analytical MPP expressions introduced in [50] are also used to correlate the MPP voltage and current with the five parameters using the Lambert *W* function, thus permitting a closed-form solution of the resulting system of equations. The equations proposed constitute a computational improvement of the method described in [2], maintaining the same levels of accuracy, at a significantly simpler and more cost efficient formulation.

In Section II of the paper, the adopted PV model and the theoretical basis for the extraction of its parameters are presented. The newly introduced correlation of the diode ideality factor and the open circuit voltage is described in Section III. The analytical method for the five parameter extraction is given in Section IV, followed by validation through simulations and outdoor measurements in Sections V and VI, respectively.

II. PV Model

A. Single-Diode Equivalent Circuit

The majority of relevant studies [2], [3], [5]–[9], [11]–[14], [16], [17], [19], [20], [22], [26], [28]–[31], [34], [39]–[43], [45], [49]–[52], rely on the single-diode electrical equivalent circuit to describe the PV cell and module, due to its simplicity and sufficient accuracy. Other works that adopt a double-diode model [15], [21], [27], [32], [35], resort to more complicated methods to determine the seven parameters of the model, without any substantial gain in accuracy. Alternative approaches not based on equivalent circuits have been also proposed, such as [53] where the Gompertz function is employed.

In Fig. 1, the equivalent circuit of the single-diode model, adopted in this paper, is depicted, comprising a photocurrent source, a diode, a series and a shunt resistance. The five parameters of the model are the value of the current source I_{ph}, the saturation current I_s and the modified diode ideality factor a of the diode, and the two resistances R_s and R_{sh}. In some studies, the shunt resistance R_{sh} [4], [10], [38], [46], [47], or even both resistances [18], [37], are neglected to simplify the model.

The equations of the model in implicit and explicit form are given below [50]:

$$I = I_{ph} - I_s\left(e^{\frac{V+IR_s}{a}} - 1\right) - \frac{V+IR_s}{R_{sh}} \tag{1}$$

$$V = R_{sh}(I_{ph}+I_s) - (R_s+R_{sh})I - aW\left\{\frac{I_s R_{sh}}{a} e^{\frac{R_{sh}(I_{ph}+I_s-I)}{a}}\right\} \tag{2}$$

For the calculation of the Lambert *W* function used in (2), the built-in function *lambertw* of MATLAB may be utilized, or the series expansions proposed in [51] may be employed for more efficient computation. Furthermore, an even simpler approximation formula is introduced in the Appendix.

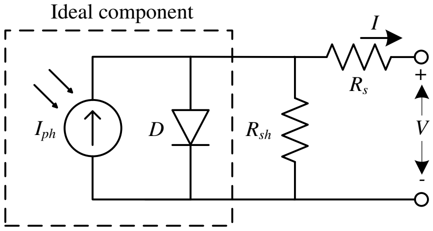

Fig. 1. Single-diode electrical equivalent circuit of the PV cell [50].

B. Theoretical Basis for the Extraction of the Five Parameters

The main concept for identifying the five parameters of the model is to select such values that the fundamental model equation (1) or (2) is satisfied at a given set of operating points.

When the entire *I-V* curve is available, this may be achieved by a curve fitting or optimization algorithm [26]–[32], [34]–[36]. However, *I-V* characteristics are not generally given in the PV module datasheets, rendering these techniques impractical for most applications.

Another approach is to form a system of equations for specific operating conditions, using only information provided in the datasheet [2]–[13], [18], [20], [37]–[39], [46]. In order to calculate the five parameters, a 5th order equation system has to be formulated. The three standard equations adopted in all studies are derived by evaluating (1) at the SC, OC and MPP operating points at STC:

$$SC: \quad I_{sc0} = I_{ph0} - I_{s0}\left(e^{\frac{I_{sc0}R_{s0}}{a_0}} - 1\right) - \frac{I_{sc0}R_{s0}}{R_{sh0}} \tag{3}$$

$$OC: \quad 0 = I_{ph0} - I_{s0}\left(e^{\frac{V_{oc0}}{a_0}} - 1\right) - \frac{V_{oc0}}{R_{sh0}} \tag{4}$$

$$MPP: I_{mp0} = I_{ph0} - I_{s0}\left(e^{\frac{V_{mp0}+I_{mp0}R_{s0}}{a_0}} - 1\right) - \frac{V_{mp0}+I_{mp0}R_{s0}}{R_{sh0}} \tag{5}$$

As a fourth equation, the derivative of power w.r.t voltage at MPP is usually set to zero [2], [3], [9]–[13], [19], [20], [38], [46]:

$$\left.\frac{dP}{dV}\right|_{MPP} = 0 \Leftrightarrow \left.\frac{dI}{dV}\right|_{MPP} = -\frac{I_{mp0}}{V_{mp0}} \tag{6}$$

Regarding the fifth equation, three main alternative approaches exist, as explained in [13] and [24]:

$$\left.\frac{dI}{dV}\right|_{sc} = -\frac{1}{R_{sh0}} \tag{7}$$

$$\left.\frac{dI}{dV}\right|_{oc} = -\frac{1}{R_{s0}} \tag{8}$$

$$\beta_{Voc} = \frac{\Delta V_{oc}}{\Delta T_c} \tag{9}$$

In [3], [6], [11], [19], [39], the slope of the *I-V* curve at SC is considered equal to the opposite reciprocal of R_{sh0}, according to (7). A similar assumption is made in [6] and [39], except for OC conditions and R_{s0} (8). A main drawback of these approaches is that (7) and (8) lack in a theoretical basis, as shown in [24], leading either to inaccuracies or to numerical solution difficulties. On the other hand, (9) states that the open circuit voltage V_{oc} varies linearly with cell temperature T_c, according to the temperature coefficient β_{Voc} [2], [4], [9]. This is generally known to be valid, at least over a limited temperature range close to 25°C, while β_{Voc} is always provided in module datasheets.

An extended discussion on the suitability of (7)-(9) to be used as the fifth equation of the system is given in [24] and [13]. In the former, it is concluded that (7) and (9) yield better results over (8), while in [13] it is shown that each alternative has its own weaknesses. For (9), in particular, not all ΔT_c values lead to a feasible solution, thus raising the need for a specific selection criterion for ΔT_c.

This shortcoming is overcome in this paper by symbolically solving (9), leading to a simple analytical expression completely independent of ΔT_c. Thereafter, this is combined with (3)-(6) to formulate a set of five equations similar to [2], but simple enough to permit symbolic solution.

III. Relation between the Modified Diode Ideality Factor and the Open Circuit Voltage

In this section, a_0 is expressed as an explicit function of V_{oc0} and the temperature coefficients. At STC, a_0 is [2]:

$$a_0 = n\frac{kT_0}{q}N_s = nV_{th0}N_s \tag{10}$$

where n and V_{th0} are the ideality factor and thermal voltage of the p-n junction respectively, T_0 the nominal temperature, k the Boltzmann constant, q the electron charge, and N_s the series connected cells in the PV unit. Since the extraction of a_0 is quite difficult, some researchers assume typical values [5], [12], while others determine its value along with the rest of the five parameters via an iterative algorithm. On the other hand, analytical expressions of a_0 in terms of the SC, OC and MPP characteristics are given in [37]–[39], but they suffer in accuracy due to the simplifications performed. In the following, a theoretically valid expression is derived by correlating the dependence of a_0 and V_{oc0} on temperature.

At open circuit, the series resistance R_s carries no current, whereas the photocurrent flows mainly through the conducting diode D and to a much smaller extent through the shunt resistance R_{sh}. Therefore, (1) may be simplified, as commonly done in the literature, to:

$$I_{ph} = I_s e^{\frac{V_{oc}}{a}} \Leftrightarrow V_{oc} = a\ln\left(\frac{I_{ph}}{I_s}\right) \tag{11}$$

If (11) is written for nominal irradiance 1000 W/m^2 and an arbitrary temperature T_c, (12) is derived using the extrapolation equations of the five parameters given in [2]:

$$(1 + a_{Isc}\Delta T_c)I_{ph0} = I_{s0}\left(\frac{T_c}{T_0}\right)^3 e^{\frac{1}{k}\left(\frac{E_{g0}}{T_0} - \frac{E_g}{T_c}\right)} e^{\frac{(1+\beta_{Voc}\Delta T_c)V_{oc0}}{a_0 T_c/T_0}} \tag{12}$$

where ΔT_c is the deviation of T_c from T_0, α_{Isc} and β_{Voc} are the normalized temperature coefficients of I_{sc} and V_{oc}, while E_g and E_{g0} are the energy gap of silicon in T_c and T_0 respectively. Thereafter, substitution of constants and rearrangement of terms in (12) leads to (details are provided in the Appendix):

$$\frac{a_0}{V_{oc0}} = \frac{1 - T_0\beta_{Voc}}{47.05 + f(\Delta T_c)}, \text{where: } f(\Delta T_c) = \left(1 + \frac{T_0}{\Delta T_c}\right)\ln\left[\frac{(1 + \Delta T_c/T_0)^3}{1 + a_{Isc}\Delta T_c}\right] \tag{13}$$

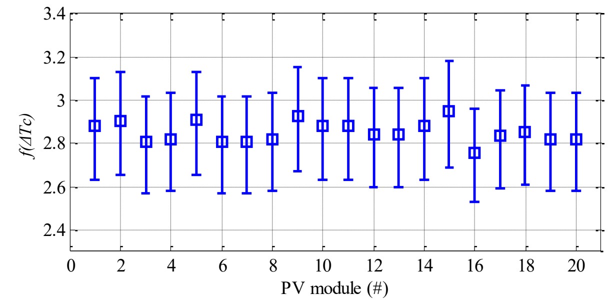

(a)

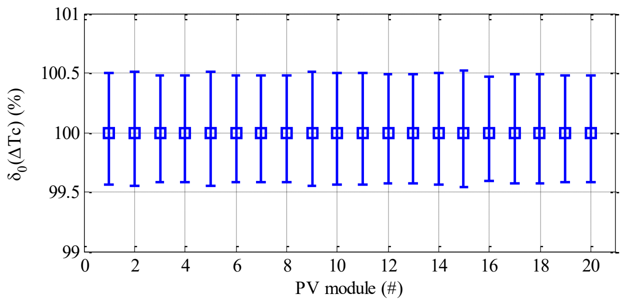

(b)

Fig. 2. Variation of: (a) term $f(\Delta T_c)$ of (13), and (b) $\delta_0=a_0/V_{oc0}$ (normalized on its value at nominal temperature T_0), over an extended range of realistic temperatures for the 20 commercial PV modules used in Section V.

This equation correlates a_0, V_{oc0}, α_{Isc} and β_{Voc} with the temperature deviation ΔT_c. At first sight, this may seem paradoxical, since the first four parameters are defined at nominal temperature and depend only on the structural characteristics of the PV module, rather than on the operating temperature. However, if $f(\Delta T_c)$ is calculated for typical values of α_{Isc} over an extended range of realistic temperatures $T_c \in [-25°C, 75°C]$, it is found that $f(\Delta T_c)$ remains close to 3, with a deviation always lower than 0.5. This is illustrated in Fig. 2(a), where the range of $f(\Delta T_c)$ variation with temperature is plotted for the 20 commercial PV modules used in Section V. $f(\Delta T_c=0)$ at nominal temperature ($T_c=T_0$) is indicated with square markers. As the deviations from the nominal values are very small compared to the constant term 47.05 in the denominator of (13), temperature clearly is not a significant parameter. This observation is further confirmed in Fig. 2(b), where (13) (i.e. the ratio of a_0 over V_{oc0}, denoted δ_0 in (14) below) is evaluated over the same temperature range for the 20 PV modules. Deviations are always less than 0.5%, therefore $f(\Delta T_c=0)$ can be reasonably used as an approximation of the actual $f(\Delta T_c)$. Hence, ignoring the temperature effect by assuming $T_c=T_0$, a relation between a_0, V_{oc0}, α_{Isc} and β_{Voc} is established via (13).

Using the typical value $f(\Delta T_c=0)$ (see Section C in the Appendix), (13) is further simplified to:

$$\delta_0 = \frac{a_0}{V_{oc0}} = \frac{1-298.15\beta_{Voc}}{50.05-298.15a_{Isc}} \tag{14}$$

where the temperature coefficients are normalized (p.u.) and signed ($\beta_{Voc}<0$, $a_{Isc}>0$).

In (14), the newly introduced coefficient δ_0, defined as the ratio of a_0 over V_{oc0} at STC, is directly related to β_{Voc} and α_{Isc}. Essentially, δ_0 correlates the dependence of a_0 and V_{oc0} on temperature, as modeled through the temperature coefficients.

Equation (14) practically constitutes a reformulation of (9), proving that the exact value of ΔT_c does not really matter, as already pointed out in [13], and replacing (9) as the fifth equation for the determination of the five parameters. At the same time, (14) ensures solution feasibility, as it always permits the determination of a_0 in a simple analytical manner, through data always provided in the module datasheet.

IV. Method for Extraction of the Five Parameters

A. Extraction at STC

As discussed above, the system of equations adopted for the determination of the five parameters at STC comprises (3)-(6) and (14). Nevertheless, the complexity of (5) and (6), which concern operation at the MPP, impedes its symbolic solution, still imposing the need for numerical/iterative computation. This is overcome by utilizing the analytical MPP expressions introduced in [50], which correlate V_{mp} and I_{mp} with the five parameters in a direct and simple way:

$$V_{mp} = (1+R_s/R_{sh})a(w-1) - R_s I_{ph}(1-1/w) \tag{15}$$

$$I_{mp} = I_{ph}(1-1/w) - a(w-1)/R_{sh} \tag{16}$$

$$V_{mp} = a(w-1) - R_s I_{mp} \tag{17}$$

where $w=W\{I_{ph}e/I_s\}$. As demonstrated in [50], the error in power estimation using these expressions is less than 0.1% at any operating condition, given that R_s remains at least two orders of magnitude smaller than R_{sh}. Similar expressions with slightly different formulation are also proposed in [54] and [55].

If (5) and (6) are replaced by (16) and (17), the system of equations is now readily solvable. In particular, if (14) is solved for a_0 and (17) for R_{s0}, (18) and (19) are derived respectively. Furthermore, solving (16) for R_{sh0} under the assumption that I_{ph0} is equal to I_{sc0}, yields (20). Moreover, neglecting the exponential term in (3), since at SC the photocurrent mainly flows through the series and shunt resistance, rather than the non-conducting diode, leads to the well-known (21). Finally, rearranging (11) to isolate I_{s0} and substituting (14), yields (22).

$$a_0 = \delta_0 V_{oc0} \tag{18}$$

$$R_{s0} = \left[a_0(w_0-1) - V_{mp0}\right]/\mathrm{I}_{mp0} \tag{19}$$

$$R_{sh0} = a_0(w_0-1)\Big/\left[I_{sc0}(1-1/w_0) - \mathrm{I}_{mp0}\right] \tag{20}$$

$$I_{ph0} = (1+R_{s0}/R_{sh0})I_{sc0} \tag{21}$$

$$I_{s0} = I_{ph0}e^{-1/\delta_0} \tag{22}$$

The parameter δ_0 is determined through (14) using the temperature coefficients, while the auxiliary term w_0 is found by substituting (11) and (14) in $w_0 = W\{I_{ph0}e/I_{s0}\}$:

$$w_0 = W\left\{e^{1/\delta_0+1}\right\} \tag{23}$$

Therefore, determination of the five parameters at STC requires first calculation of the coefficient δ_0 using (14), and then application of (23) to determine the term w_0. Thereafter, the expressions (18)-(22) are sequentially evaluated, in this order: first (18) to calculate a_0, then (19) and (20) to acquire R_{s0} and R_{sh0}, subsequently (21) to determine I_{ph0} and finally (22) for I_{s0}. It is a purely analytical method, simple and easy to implement, as it relies only on information found in the module datasheet, while it provides accurate results, as shown in the following sections.

B. Extraction at other Operating Conditions

Input data may often refer to operating conditions other than STC, such as normal operating cell temperature (NOCT) or study-case specific conditions. As shown in the following, (18)-(22) can still be applied, for arbitrary irradiance and temperature.

First, the ratio of a over V_{oc}, denoted as δ, is found for the general case. Provided that a is linearly dependent on temperature and it is not affected by irradiance [2], δ is expressed as:

$$\delta = \frac{a}{V_{oc}} \overset{[2]}{=} \frac{a_0 T_c / T_0}{V_{oc}} \overset{(14)}{=} \delta_0 \frac{V_{oc0}}{V_{oc}} \frac{T_c}{T_0} \tag{24}$$

where temperatures T_c and T_0 are expressed in K. Therefore, if the characteristic operating points SC, OC and MPP are known at the study-case conditions, as well as at STC from the datasheet, the extraction methodology involves first evaluation of (14) for δ_0, then (24) for δ. Thereafter, $w = W\left\{e^{1/\delta+1}\right\}$ is calculated and (18)-(22) are evaluated, noting that all terms refer to the specific operating conditions, rather than to STC.

V. Validation and Comparative Assessment through Simulations

In this section, the model introduced is validated through simulations in MATLAB. The numerical method of De Soto [2] is adopted as a reference, since it is a well-established model in the literature and it is based on the same theoretical assumptions as the proposed equations. This way, it is shown that the latter provide practically the same accuracy, but in a simpler and straightforward manner.

A. Validation of the Coefficient δ_0

In order to verify the theoretical analysis of Section III and the validity of (14), the ratio of a_0 over V_{oc0} is studied at STC for 20 commercial PV modules given in Table I. This ratio is first calculated via the numerical method of De Soto [2], and then it is compared to the coefficient δ_0 as determined through (14). In Fig. 3, the reference values of the ratio are indicated with blue square markers, while the estimated values using (14) with red cross markers. As shown, the deviations are negligible, presenting rms and maximum errors 0.07% and less than 0.1% respectively.

Moreover, it is worth noting that δ_0 is always very close to 0.04 (green line). This may be explained if the near-zero values of α_{Isc} and the limited range of β_{Voc} (close to -0.003) are considered. Substituting these values in (14) yields $\delta_0 \approx 0.04$, which therefore represents its typical value.

B. Validation of the Five Parameter Extraction Method

In the following, the proposed extraction method is applied and compared to other explicit approaches found in the literature in terms of accuracy and computational effort. Specifically, the explicit techniques presented in [37]–[39], which also rely *only* on datasheet information, are implemented and denoted by the names of their respective main authors: *Saloux*, *Khezzar,* and *Bai*. The simulations

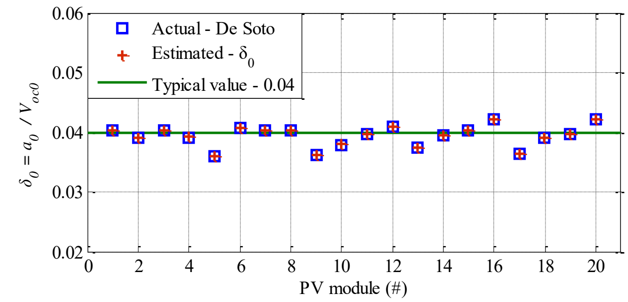

Fig. 3. Parameter δ_0 (ratio of a_0 over V_{oc0}) as calculated using the method of De Soto and through (14) for 20 commercial PV modules.

presented correspond to extended ranges of irradiance (100 to 1000 W/m^2 with a step of 50 W/m^2) and temperature variations (-25 to 75°C with a step of 5°C), while they are repeated for the 20 commercial PV modules, leading to 7980 scenarios in total.

The simulation methodology adopted consists of the following steps. First, the five parameters are determined at STC through the *DeSoto* model for the study-case module and then extrapolated to the actual operating conditions [2]. Thereafter, the *I-V* curve is constructed and the three characteristic operating points SC, OC and MPP are recorded. The latter are considered as the input data which are fed to the *Proposed* and the other three explicit approaches. After evaluating the five parameters using each of the alternative models, the *I-V* characteristic is reconstructed and is compared to the reference one by *DeSoto*. As a measure of the achieved accuracy, the normalized root mean squared deviation (NRMSD) of the entire *I-V* curve from the reference one is used, in the same way as in [17].

In order to evaluate the estimation accuracy of the *Proposed* method, the NRMSD distribution over the simulated irradiance and temperature ranges is recorded in Fig. 4. Each error value corresponds to the mean NRMSD for all PV modules considered, presenting global rms and maximum errors of 0.43% and less than 1%, respectively. It is worth noting that maximum deviation is observed at the highest values of irradiance and temperature. This is because of the MPP expressions (15)-(17) adopted, which slightly underestimate V_{mp} and overestimate I_{mp} in these conditions [50].

In Table I, the rms and maximum NRMSD using each explicit approach are shown for every PV module considered. The *Proposed* method shows best performance among all

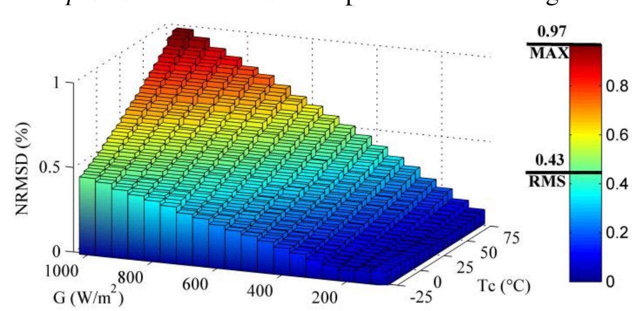

Fig. 4. Distribution of NRMSD over the entire range of irradiance and temperature, using the *Proposed* technique as compared to the *DeSoto* method. NRMSD values plotted represent the mean for the 20 PV modules studied.

TABLE I
ESTIMATION ERROR OF THE EXPLICIT METHODS AS COMPARED TO THE *DESOTO* APPROACH FOR 20 DIFFERENT COMMERCIAL PV MODULES

PV module	NRMSD (%) of the explicit methods							
	Saloux		*Khezzar*		*Bai*		*Proposed*	
	RMS	MAX	RMS	MAX	RMS	MAX	RMS	MAX
Aleo s18-235	**3.49**	7.61	**0.59**	1.25	**1.34**	2.07	**0.42**	0.97
Bosch M60s-245	**3.48**	7.39	**0.39**	0.72	**1.39**	2.10	**0.44**	0.98
Canadian Solar CS6P 250	**3.04**	6.87	**0.95**	2.02	**1.27**	2.06	**0.31**	0.77
Conergy PowerPlus 190P	**3.13**	6.79	**0.74**	1.59	**1.28**	1.99	**0.34**	0.80
Day4 Energy 60MC-I	**3.30**	7.09	**0.94**	1.96	**1.16**	1.67	**0.33**	0.75
ET Zero-rack 240	**3.90**	8.61	**0.54**	1.12	**1.38**	2.17	**0.50**	1.14
LDK 235 P-20	**2.77**	6.25	**0.76**	1.58	**1.31**	2.13	**0.29**	0.71
Perllight PLM-250P-60	**2.14**	4.40	**2.20**	4.10	**1.45**	2.74	**0.33**	0.51
REC 250PE	**3.50**	7.69	**1.32**	2.76	**1.17**	2.06	**0.32**	0.75
Renesola Virtus II 250	**3.36**	7.12	**0.67**	1.46	**1.24**	1.88	**0.37**	0.85
SCHOTT Perform 240	**3.09**	7.12	**1.81**	3.62	**1.28**	2.45	**0.28**	0.58
Sharp NU-E240 (J5)	**3.30**	7.43	**2.07**	4.20	**1.32**	2.79	**0.32**	0.61
Silcio SE250	**3.84**	8.23	**0.56**	1.21	**1.25**	1.90	**0.46**	1.02
Solea SM 190	**3.33**	7.52	**1.44**	2.98	**1.22**	2.15	**0.30**	0.72
Sopray SR 245	**2.57**	5.66	**1.08**	2.19	**1.26**	1.94	**0.24**	0.56
Sunmodule SW 240	**2.69**	5.70	**0.40**	0.88	**1.59**	2.38	**0.36**	0.82
Sunpower E19-240	**2.50**	5.50	**1.25**	2.45	**1.21**	1.85	**0.20**	0.48
Upsolar UP-M240P	**3.29**	6.85	**0.35**	0.81	**1.53**	2.24	**0.45**	0.95
Yingli YGE 250P-29b	**3.69**	7.88	**0.62**	1.34	**1.31**	2.00	**0.45**	1.03
Yingli YL-165	**4.05**	9.48	**2.60**	5.18	**1.38**	3.28	**0.44**	0.76
OVERALL	**3.26**	9.48	**1.24**	5.18	**1.32**	3.28	**0.37**	1.14

explicit techniques. It is worth noting that the *Saloux*, *Khezzar* and *Bai* methods all present maximum errors for the YL165 module, which is the oldest study-case module, with significant series and shunt losses. Moreover, it is worth mentioning that if the simple formula (26) is employed for the Lambert W function (see Appendix) instead of a series expansions [51], the resulting error increment does not exceed 0.05%, rendering it a useful alternative for an even simpler implementation without any marked reduction in accuracy.

As far as the execution time is concerned, the computational effort required by the *DeSoto* method and each of the explicit models is shown in absolute and normalized form in Table II (all simulations conducted on the same PC with a 3.4-GHz CPU and 6.00-GB RAM). The *Proposed* technique is slightly more time-consuming compared to the other analytical models, due to the Lambert W function evaluation. This overhead is drastically reduced if the simplified formula (26) is employed. Nonetheless, all explicit methods present practically the same level of performance compared to the *DeSoto* model, which is around three to four orders of magnitude slower. In conclusion, the *Proposed* method presents the same accuracy as the reference *DeSoto* model, but at a significantly simpler and computationally more efficient implementation.

VI. EXPERIMENTAL VALIDATION THROUGH MEASUREMENTS

TABLE II
EXECUTION TIME OF THE *DESOTO* AND THE EXPLICIT METHODS

Method	Execution time (μs) per scenario	Execution time normalized on the *Proposed* method
DeSoto	10805.4	3178.06
Saloux	1.4	0.41
Khezzar	1.5	0.44
Bai	2.5	0.74
Proposed	**3.4**	**1.00**
***Proposed* (*simple W*)**	1.9	0.59

TABLE III
PV MODULES USED IN THE EXPERIMENTAL VALIDATION

Model	Type	Cells	I_{sc0} (A)	V_{oc0} (V)	I_{mp0} (A)	V_{mp0} (V)
Conergy PowerPlus 190PC	poly	48	8.61	29.52	8.09	23.87
Day4 Energy 60MC-I	poly	60	8.58	37.32	8.08	30.29
Perllight PLM-250P-60	poly	60	8.49	37.58	7.88	31.73
Solea SM 190	mono	72	5.73	44.18	5.33	35.65
Yingli YL-165	poly	48	7.90	29.0	7.17	23.0

To further verify the validity of the expressions introduced in this paper, outdoor measurements have been taken for five commercial PV modules at three different operating conditions. The properties of the study-case modules are given in Table III. The *I-V* characteristics and the actual irradiance and temperature were recorded using the *Amprobe Solar-4000 Analyzer* PV tracer. The irradiance sensor of the equipment employs two PV cells, one monocrystalline and one polycrystalline, while the temperature meter features an infrared sensor. The validation procedure involves first recording of the *I-V* curve, then locating the SC, OC and MPP operating points and using them as input data to the four explicit methods, in order to evaluate the five parameters and reconstruct the *I-V* characteristic for comparison with the original measured one.

In Fig. 5, the measured *I-V* curve is depicted for an indicative case, along with the simulated characteristics derived from the four explicit models. As shown in the upper zoom-box, the *Saloux* and *Khezzar* methods overestimate the current in the region between SC and MPP, due to neglecting the shunt resistance in the model, whereas the *Bai* technique underestimates the current in this region, because of the assumptions made for estimating the slope at SC. In the region between MPP and OC (lower zoom-box in Fig. 5), the *Saloux* method noticeably deviates from the measurements due to the simplifications assumed (series and shunt resistances are ignored – slope at MPP is considered equal to V_{oc}/I_{sc}), while the other two explicit approaches perform satisfactorily. The *Proposed* method provides excellent results over the entire range of the *I-V* characteristic.

This is further confirmed in Table IV, where the NRMSD of the four analytical models is shown for each case. The *Saloux* method presents errors up to almost 10%, while the *Khezzar* and *Bai* methods perform better, still presenting rms errors higher than the maximum NRMSD recorded for the *Proposed* model. The rms error of the latter is only slightly higher than 1%, proving sufficiently accurate in practice, as well.

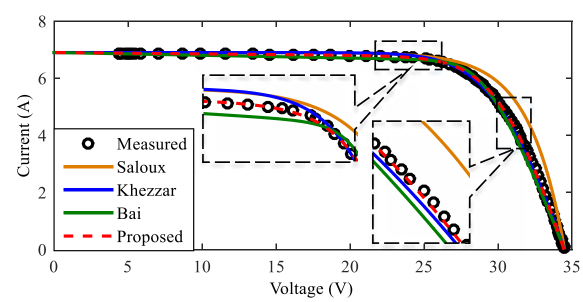

Fig. 5. Measured and simulated *I-V* curves using the analytical methods for an indicative case (Perllight PLM-250P-60 module at 805 W/m^2 – 45°C).

TABLE IV

ESTIMATION ACCURACY OF THE EXPLICIT METHODS BASED ON MEASUREMENTS ON FIVE COMMERCIAL PV MODULES

PV module	NRMSD (%) compared to measured *I-V*			
Operating conditions	***Saloux***	***Khezzar***	***Bai***	***Proposed***
Conergy PowerPlus 190PC				
917 W/m² – 57°C	5.91	1.90	3.13	1.15
857 W/m² – 56°C	6.11	1.78	3.00	0.94
465 W/m² – 58°C	1.74	2.60	1.83	1.75
Day4 Energy 60MC-I				
906 W/m² – 47°C	7.12	2.10	3.21	1.76
743 W/m² – 42°C	5.44	1.12	2.43	1.34
518 W/m² – 39°C	3.05	0.80	1.56	1.53
Perllight PLM-250P-60				
902 W/m² – 40°C	9.44	2.22	3.06	0.54
805 W/m² – 45°C	8.51	1.54	2.58	0.66
500 W/m² – 47°C	5.10	3.23	1.94	1.70
Solea SM 190				
930 W/m² – 45°C	3.92	0.38	1.55	0.72
772 W/m² – 40°C	2.59	1.03	1.27	0.72
544 W/m² – 35°C	2.26	0.49	1.82	1.22
Yingli YL-165				
976 W/m² – 58°C	4.86	1.65	2.59	0.91
593 W/m² – 47°C	2.60	2.27	3.26	0.59
437 W/m² – 43°C	4.25	0.64	2.21	1.07
OVERALL RMS	**5.34**	**1.78**	**2.45**	**1.18**
OVERALL MAXIMUM	**9.44**	**3.23**	**3.26**	**1.76**

It is worth mentioning that temperature measurements may present significant inaccuracies. However, this does not affect the validation of the four explicit models, since they rely on the SC, OC and MPP voltage and current measurements, in which the temperature effect is already included, while the impact on the modified diode ideality factor in the *Proposed* and *Saloux* methods is only secondary.

VII. CONCLUSION

In this paper, a new coefficient for the single-diode PV model was first introduced, denoted as δ, which correlates the modified diode ideality factor and the open circuit voltage with the temperature coefficients. This coefficient was used to derive an analytical expression for the diode ideality factor of the model using only datasheet information.

A set of analytical expressions were then developed to calculate the five parameters of the single-diode model in a straightforward, simple and cost-efficient manner. The input data of these equations are the voltage and current at short-circuit, open-circuit and maximum power conditions, as well as the temperature coefficients, while the equations are applicable at any operating conditions. The accuracy of the method was validated through simulations and outdoor measurements, by comparison to other explicit approaches available in the literature.

The method introduced constitutes a computational improvement of the model of De Soto [2], presenting practically the same accuracy, with significant gains in robustness, efficiency and ease of implementation. These properties render the proposed expressions a useful tool for PV modeling, especially in applications where different PV modules need to be studied at various operating conditions.

APPENDIX

A. Simple Approximation Formula of the Lambert W Function

The Lambert *W* function $W\{x\}$ is the inverse of the equation $we^{w}=x$ and it cannot be expressed in terms of elementary functions. Generally, iterative algorithms are used in MATLAB and other computational platforms, but more efficient calculation is possible when series expansions are employed instead, such as the ones proposed in [51]. An even simpler formula is introduced in this paper, utilizing the work of [56]. As explained therein, the Lambert *W* function of $e^{\lambda+B}$ may be approximated by:

$$W\left\{e^{\lambda+\mathrm{B}}\right\}=\lambda\left(1-\frac{\ln\lambda+\mathrm{B}}{\lambda+1}\right) \tag{25}$$

where λ is a large positive number and B is a constant. If B is set to zero and λ to $\ln(x)$, $W\{x\}$ is then expressed as:

$$W\{x\}=\ln(x)\left[1-\frac{\ln(\ln(x))}{\ln(x)+1}\right] \tag{26}$$

The above expression provides a sufficiently accurate approximation of $W\{x\}$ for $x\geq 2$, whose error is always less than 1.5%. Thus, it provides a simpler and more cost-efficient implementation, compared to other approaches, when x does not take small values.

B. Derivation of (13)

In order to simplify (12), (11) is applied at STC to express I_{ph0} as in (27), the ratio T_c/T_0 is rewritten according to (28), while the term $(E_{g0}/T_0-E_g/T_c)/k$ is reformulated using the extrapolation equation of the energy gap of silicon: $E_g=E_{g0}(1-0.0002677\Delta T_c)$ [2], and the constant values E_{g0}=1.7958e-19 J and k=1.381e-23 J/k, leading to (29):

$$I_{ph0}=I_{s0}e^{V_{oc0}/a_0} \tag{27}$$

$$T_c/T_0=\Delta T_c/T_0+1 \tag{28}$$

$$\frac{1}{k}\left(\frac{E_{g0}}{T_0}-\frac{E_g}{T_c}\right)=47.05\frac{\Delta T_c}{\Delta T_c+T_0} \tag{29}$$

Substitution of (27)-(29) in (12) yields:

$$(1+a_{Isc}\Delta T_c)\,\cancel{I_{s0}}\,e^{\frac{V_{oc0}}{a_0}}=\cancel{I_{s0}}\left(\frac{\Delta T_c}{T_0}+1\right)^3 e^{\frac{47.05\Delta T_c}{\Delta T_c+T_0}}\,e^{\frac{(1+\beta_{Voc}\Delta T_c)V_{oc0}}{a_0(\Delta T_c/T_0+1)}} \tag{30}$$

As the terms I_{s0} in the right and left hand side of (30) cancel out, the following relation can be derived after some manipulation:

$$\frac{a_0}{V_{oc0}}=\frac{1-T_0\beta_{Voc}}{47.05+\underbrace{\left(1+\frac{T_0}{\Delta T_c}\right)\ln\left[\frac{(1+\Delta T_c/T_0)^3}{1+a_{Isc}\Delta T_c}\right]}_{f(\Delta T_c)}} \tag{31}$$

Apparently, (31) is identical to (13), while it is worth noting that the temperature effect is limited only to the term $f(\Delta T_c)$ in the denominator.

C. Calculation of a Typical Value for $f(\Delta T_c)$

As discussed in Section III, the term $f(\Delta T_c)$ in (13) varies in a limited range, for typical values of α_{Isc} under any realistic temperature. In order to handle $f(\Delta T_c)$ as a constant, its value at the nominal temperature T_0 is calculated and considered as typical. Since $f(\Delta T_c)$ is not defined in T_0 (ΔT_c=0), the corresponding limit is evaluated:

$$
\begin{aligned}
&\lim_{\Delta T_c \to 0} f(\Delta T_c) = \lim_{\Delta T_c \to 0}\left[\left(1+\frac{T_0}{\Delta T_c}\right)\ln\left(\frac{\left(1+\Delta T_c/T_0\right)^3}{1+a_{Isc}\Delta T_c}\right)\right] = \\
&3\ln\left[\lim_{\Delta T_c \to 0}\left(\left(1+\Delta T_c/T_0\right)^{1+\frac{T_0}{\Delta T_c}}\right)\right] - \ln\left[\lim_{\Delta T_c \to 0}\left(\left(1+a_{Isc}\Delta T_c\right)^{1+\frac{T_0}{\Delta T_c}}\right)\right] = \\
&3\ln\left[\cancel{\lim_{\Delta T_c \to 0}\left(1+\Delta T_c/T_0\right)^1}\right] + 3\ln\left[\lim_{\Delta T_c \to 0}\left(1+\Delta T_c/T_0\right)^{T_0/\Delta T_c}\right] \\
&-\ln\left[\cancel{\lim_{\Delta T_c \to 0}\left(1+a_{Isc}\Delta T_c\right)^1}\right] - \ln\left[\lim_{\Delta T_c \to 0}\left(1+a_{Isc}\Delta T_c\right)^{T_0/\Delta T_c}\right]
\end{aligned} \tag{32}
$$

The crossed-out terms above are equal to zero, while considering the definition of the exponential function:

$$
e^x = \lim_{n \to \infty}\left(1+\frac{x}{n}\right)^n = \lim_{n \to 0}\left(1+xn\right)^{\frac{1}{n}} \tag{33}
$$

the two remaining terms in (32) are expressed as:

$$
\begin{aligned}
&3\ln\left[\lim_{\Delta T_c \to 0}\left(1+\Delta T_c/T_0\right)^{T_0/\Delta T_c}\right] = 3\ln(e^1) = 3 \\
&\ln\left[\lim_{\Delta T_c \to 0}\left(1+a_{Isc}\Delta T_c\right)^{T_0/\Delta T_c}\right] = \ln\left(e^{a_{Isc}T_0}\right) = a_{Isc}T_0
\end{aligned} \tag{34}
$$

Thus, $\lim_{\Delta T_c \to 0} f(\Delta T_c) = 3 - a_{Isc}T_0$, which is then substituted in (13), eventually leading to (14).

References

[1] E. I. Batzelis, P. S. Georgilakis, and S. A. Papathanassiou, "Energy models for photovoltaic systems under partial shading conditions: a comprehensive review," *IET Renew. Power Gener.*, vol. 9, no. 4, pp. 340–349, May 2015.

[2] W. De Soto, S. A. Klein, and W. A. Beckman, "Improvement and validation of a model for photovoltaic array performance," *Sol. Energy*, vol. 80, no. 1, pp. 78–88, Jan. 2006.

[3] D. Sera, R. Teodorescu, and P. Rodriguez, "PV panel model based on datasheet values," in *Proc. 2007 IEEE Int. Symp. Ind. Electron.*, Caixanova - Vigo, Spain, Jun. 2007, pp. 2392–2396.

[4] R. Chenni, M. Makhlouf, T. Kerbache, and A. Bouzid, "A detailed modeling method for photovoltaic cells," *Energy*, vol. 32, no. 9, pp. 1724–1730, Sep. 2007.

[5] M. G. Villalva, J. R. Gazoli, and E. R. Filho, "Comprehensive approach to modeling and simulation of photovoltaic arrays," *IEEE Trans. Power Electron.*, vol. 24, no. 5, pp. 1198–1208, May 2009.

[6] V. Lo Brano, A. Orioli, G. Ciulla, and A. Di Gangi, "An improved five-parameter model for photovoltaic modules," *Sol. Energy Mater. Sol. Cells*, vol. 94, no. 8, pp. 1358–1370, Aug. 2010.

[7] C. Carrero, D. Ramírez, J. Rodríguez, and C. A. Platero, "Accurate and fast convergence method for parameter estimation of PV generators based on three main points of the I–V curve," *Renew. Energy*, vol. 36, no. 11, pp. 2972–2977, Nov. 2011.

[8] F. Ghani, M. Duke, and J. Carson, "Numerical calculation of series and shunt resistances and diode quality factor of a photovoltaic cell using the Lambert W-function," *Sol. Energy*, vol. 91, pp. 422–431, May 2013.

[9] S. Lun, C. Du, G. Yang, S. Wang, T. Guo, J. Sang, and J. Li, "An explicit approximate I–V characteristic model of a solar cell based on padé approximants," *Sol. Energy*, vol. 92, pp. 147–159, Jun. 2013.

[10] M. Averbukh, S. Lineykin, and A. Kuperman, "Obtaining small photovoltaic array operational curves for arbitrary cell temperatures and solar irradiation densities from standard conditions data," *Prog. Photovolt.: Res. Appl.*, vol. 21, no. 5, pp. 1016–1024, Aug. 2013.

[11] K. Ding, J. Zhang, X. Bian, and J. Xu, "A simplified model for photovoltaic modules based on improved translation equations," *Sol. Energy*, vol. 101, pp. 40–52, Mar. 2014.

[12] L. Peng, Y. Sun, and Z. Meng, "An improved model and parameters extraction for photovoltaic cells using only three state points at standard test condition," *J. Power Sources*, vol. 248, pp. 621–631, Feb. 2014.

[13] A. Laudani, F. Riganti Fulginei, and A. Salvini, "Identification of the one-diode model for photovoltaic modules from datasheet values," *Sol. Energy*, vol. 108, pp. 432–446, Oct. 2014.

[14] A. Orioli and A. Di Gangi, "A procedure to calculate the five-parameter model of crystalline silicon photovoltaic modules on the basis of the tabular performance data," *Appl. Energy*, vol. 102, pp. 1160–1177, Feb. 2013.

[15] A. A. Elbaset, H. Ali, and M. Abd-El Sattar, "Novel seven-parameter model for photovoltaic modules," *Sol. Energy Mater. Sol. Cells*, vol. 130, pp. 442–455, Nov. 2014.

[16] B. Subudhi and R. Pradhan, "Characteristics evaluation and parameter extraction of a solar array based on experimental analysis," in *Proc. 2011 IEEE 9th Int. Conf. Power Electron. Drive Syst.*, Singapore, Singapore, Dec. 2011, pp. 340–344.

[17] Y. A. Mahmoud, W. Xiao, and H. H. Zeineldin, "A parameterization approach for enhancing PV model accuracy," *IEEE Trans. Ind. Electron.*, vol. 60, no. 12, pp. 5708–5716, Dec. 2013.

[18] Y. Mahmoud, W. Xiao, and H. H. Zeineldin, "A simple approach to modeling and simulation of photovoltaic modules," *IEEE Trans. Sustain. Energy*, vol. 3, no. 1, pp. 185–186, Jan. 2012.

[19] A. Chatterjee, A. Keyhani, and D. Kapoor, "Identification of Photovoltaic Source Models," *IEEE Trans. Energy Convers.*, vol. 26, no. 3, pp. 883–889, Sep. 2011.

[20] Y. Mahmoud and E. F. El-Saadany, "A photovoltaic model with reduced computational time," *IEEE Trans. Ind. Electron.*, vol. 62, no. 6, pp. 3534–3544, Jun. 2014.

[21] B. C. Babu and S. Gurjar, "A novel simplified two-diode model of photovoltaic (PV) module," *IEEE J. Photovoltaics*, vol. 4, no. 4, pp. 1156–1161, Jul. 2014.

[22] F. Caracciolo, E. Dallago, D. G. Finarelli, A. Liberale, and P. Merhej, "Single-variable optimization method for evaluating solar cell and solar module parameters," *IEEE J. Photovoltaics*, vol. 2, no. 2, pp. 173–180, Apr. 2012.

[23] S. Lineykin, M. Averbukh, and A. Kuperman, "Issues in modeling amorphous silicon photovoltaic modules by single-diode equivalent circuit," *IEEE Trans. Ind. Electron.*, vol. 61, no. 12, pp. 6785–6793, Dec. 2014.

[24] T. Ma, H. Yang, and L. Lu, "Development of a model to simulate the performance characteristics of crystalline silicon photovoltaic modules/strings/arrays," *Sol. Energy*, vol. 100, pp. 31–41, Feb. 2014.

[25] S. Shongwe and M. Hanif, "Comparative analysis of different single-diode PV modeling methods," *IEEE J. Photovoltaics*, vol. 5, no. 3, pp. 938–946, May 2015.

[26] T. Ikegami, T. Maezono, F. Nakanishi, Y. Yamagata, and K. Ebihara, "Estimation of equivalent circuit parameters of PV module and its application to optimal operation of PV system," *Sol. Energy Mater. Sol. Cells*, vol. 67, no. 1–4, pp. 389–395, Mar. 2001.

[27] M. Haouari-Merbah, M. Belhamel, I. Tobías, and J. M. Ruiz, "Extraction and analysis of solar cell parameters from the illuminated current–voltage curve," *Sol. Energy Mater. Sol. Cells*, vol. 87, no. 1–4, pp. 225–233, May 2005.

[28] A. Ortiz-Conde, F. García Sánchez, and J. Muci, "New method to extract the model parameters of solar cells from the explicit analytic solutions of their illuminated I-V characteristics," *Sol. Energy Mater. Sol. Cells*, vol. 90, no. 3, pp. 352–361, Feb. 2006.

[29] L. H. I. Lim, Z. Ye, J. Ye, D. Yang, and H. Du, "A linear identification of diode models from single I-V characteristics of PV panels," *IEEE Trans. Ind. Electron.*, vol. 62, no. 7, pp. 4181–4193, Jul. 2015.

[30] M. Zagrouba, A. Sellami, M. Bouaïcha, and M. Ksouri, "Identification of PV solar cells and modules parameters using the genetic algorithms: Application to maximum power extraction," *Sol. Energy*, vol. 84, no. 5, pp. 860–866, May 2010.

[31] H. Fathabadi, "Novel neural-analytical method for determining silicon/plastic solar cells and modules characteristics," *Energy Convers. Manag.*, vol. 76, pp. 253–259, Dec. 2013.

[32] M. R. AlRashidi, M. F. AlHajri, K. M. El-Naggar, and A. K. Al-Othman, "A new estimation approach for determining the I–V characteristics of solar cells," *Sol. Energy*, vol. 85, no. 7, pp. 1543–1550, Jul. 2011.

[33] J. J. Soon and K.-S. Low, "Photovoltaic model identification using particle swarm optimization with inverse barrier constraint," *IEEE*

Trans. Power Electron., vol. 27, no. 9, pp. 3975–3983, Sep. 2012.
[34] K. Ishaque and Z. Salam, "An improved modeling method to determine the model parameters of photovoltaic (PV) modules using differential evolution (DE)," *Sol. Energy*, vol. 85, no. 9, pp. 2349–2359, Sep. 2011.
[35] A. Askarzadeh and A. Rezazadeh, "Extraction of maximum power point in solar cells using bird mating optimizer-based parameters identification approach," *Sol. Energy*, vol. 90, pp. 123–133, Apr. 2013.
[36] O. Hachana, K. E. Hemsas, G. M. Tina, and C. Ventura, "Comparison of different metaheuristic algorithms for parameter identification of photovoltaic cell/module," *J. Renew. Sustain. Energy*, vol. 5, no. 5, Sep. 2013.
[37] E. Saloux, A. Teyssedou, and M. Sorin, "Explicit model of photovoltaic panels to determine voltages and currents at the maximum power point," *Sol. Energy*, vol. 85, no. 5, pp. 713–722, May 2011.
[38] R. Khezzar, M. Zereg, and A. Khezzar, "Modeling improvement of the four parameter model for photovoltaic modules," *Sol. Energy*, vol. 110, pp. 452–462, Dec. 2014.
[39] J. Bai, S. Liu, Y. Hao, Z. Zhang, M. Jiang, and Y. Zhang, "Development of a new compound method to extract the five parameters of PV modules," *Energy Convers. Manag.*, vol. 79, pp. 294–303, Mar. 2014.
[40] J. C. H. Phang, D. S. H. Chan, and J. R. Phillips, "Accurate analytical method for the extraction of solar cell model paramaters," *Electron. Lett.*, vol. 20, no. 10, pp. 406–408, Jan. 1984.
[41] M. A. De Blas, J. L. Torres, E. Prieto, and A. García, "Selecting a suitable model for characterizing photovoltaic devices," *Renew. Energy*, vol. 25, no. 3, pp. 371–380, Mar. 2002.
[42] F. Khan, S.-H. Baek, Y. Park, and J. H. Kim, "Extraction of diode parameters of silicon solar cells under high illumination conditions," *Energy Convers. Manag.*, vol. 76, pp. 421–429, Dec. 2013.
[43] J. Cubas, S. Pindado, and M. Victoria, "On the analytical approach for modeling photovoltaic systems behavior," *J. Power Sources*, vol. 247, pp. 467–474, Feb. 2014.
[44] F. J. Toledo and J. M. Blanes, "Geometric properties of the single-diode photovoltaic model and a new very simple method for parameters extraction," *Renew. Energy*, vol. 72, pp. 125–133, Dec. 2014.
[45] H. Saleem and S. Karmalkar, "An analytical method to extract the physical parameters of a solar cell from four points on the illuminated J-V curve," *IEEE Electron Device Lett.*, vol. 30, no. 4, pp. 349–352, Apr. 2009.
[46] B. Aldwane, "Modeling, simulation and parameters estimation for Photovoltaic module," in *Proc. 2014 1st Int. Conf. Green Energy ICGE 2014*, Sfax, Tunisia, Mar. 2014, pp. 101–106.
[47] J. M. Blanes, F. J. Toledo, S. Montero, and A. Garrigós, "In-site real-time photovoltaic I–V curves and maximum power point estimator," *IEEE Trans. Power Electron.*, vol. 28, no. 3, pp. 1234–1240, Mar. 2013.
[48] D. S. H. Chan, J. R. Phillips, and J. C. H. Phang, "A comparative study of extraction methods for solar cell model parameters," *Solid State Electron.*, vol. 29, no. 3, pp. 329–337, Mar. 1986.
[49] A. Hadj Arab, F. Chenlo, and M. Benghanem, "Loss-of-load probability of photovoltaic water pumping systems," *Sol. Energy*, vol. 76, no. 6, pp. 713–723, Jan. 2004.
[50] E. I. Batzelis, G. E. Kampitsis, S. A. Papathanassiou, and S. N. Manias, "Direct MPP calculation in terms of the single-diode PV model parameters," *IEEE Trans. Energy Convers.*, vol. 30, no. 1, pp. 226–236, Mar. 2015.
[51] E. I. Batzelis, I. A. Routsolias, and S. A. Papathanassiou, "An explicit PV string model based on the Lambert W function and simplified MPP expressions for operation under partial shading," *IEEE Trans. Sustain. Energy*, vol. 5, no. 1, pp. 301–312, Jan. 2014.
[52] Y. Mahmoud and E. El-Saadany, "Accuracy improvement of the ideal PV model," *IEEE Trans. Sustain. Energy*, vol. 6, no. 3, pp. 909–911, Jul. 2015.
[53] A. Molina-Garcia, J. Guerrero-Perez, M. C. Bueso, M. Kessler, and E. Gomez-Lazaro, "A new solar module modeling for PV applications based on a symmetrized and shifted Gompertz model," *IEEE Trans. Energy Convers.*, vol. 30, no. 1, pp. 51–59, Mar. 2015.
[54] G. Farivar, B. Asaei, and S. Mehrnami, "An analytical solution for tracking photovoltaic module MPP," *IEEE J. Photovoltaics*, vol. 3, no. 3, pp. 1053–1061, Jul. 2013.
[55] A. Kuperman, "Comments on 'An analytical solution for tracking photovoltaic module MPP,'" *IEEE J. Photovoltaics*, vol. 4, no. 2, pp. 734–735, Mar. 2014.
[56] W. Borsch-Supan, "On the Evaluation of the Function φ(λ) for Real Values of λ," *J. Res.*, vol. 65B, no. 4, pp. 245–250, Oct. 1961.

Efstratios I. Batzelis (S'14) received the Diploma in Electronic & Computer Engineering from the Technical University of Crete (TUC), Chania, Greece, in 2009, and his M.Sc. degree on Energy Production & Management from the National Technical University of Athens (NTUA), Athens, Greece, in 2012, where he is currently working towards the Ph.D. degree.

His current research interests include renewable energy technologies and power electronics, especially photovoltaic system design and simulation under mismatched operation.

Stavros A. Papathanassiou (S'93–M'98–SM'10) received the Diploma degree in Electrical Engineering and the Ph.D. degree from the National Technical University of Athens (NTUA), Athens, Greece, in 1991 and 1997, respectively.

He was with the Distribution Division, Public Power Corporation of Greece, engaged in power quality and distributed generation (DG) studies. In 2002, he joined the Electric Power Division, NTUA, where he is currently an Associate Professor. From 2009 to 2012, he was a Member of the Board of the Hellenic Transmission System Operator. His research interests are in the field of renewable energy sources (RES) and DG, including wind turbine and PV technology, storage applications and integration of DG to the grid.